View metadata, citation and similar papers at core.ac.uk
brought to you by CORE
provided by CERN Document Server

High Q^2 results from HERA

Georges Cozzika
CE-Saclay, DSM/DAPNIA/SPP
F-91191 Gif-sur-Yvette, France
E-mail : cozzika@hep.saclay.cea.fr

(On behalf of the H1 and ZEUS Collaborations)

Abstract

Measurements of deep inelastic ep scattering at high Q^2 performed at HERA between 1994 and early 2000 by the H1 and ZEUS collaborations are presented. The data are compared to expectations from the Standard Model and are used to set constraints on various extension models. In the second part, the previously reported observation of events with an isolated high P_T lepton and missing transverse momentum is discussed, the observed rates and event characteristics being compared to the expectations from Standard Model W production.

1 Introduction

At the HERA ep collider at DESY measurements of inclusive deep inelastic scattering (DIS) cross sections in Neutral Current (NC) and Charged Current (CC) processes have been performed. These offer a unique possibility to probe the proton at very small distances and to investigate DIS in a region where electromagnetic and weak interactions are of comparable strength.

The luminosity delivered by HERA from 1994 to 2000 has allowed each of the experiments H1 and ZEUS to accumulate about 100 pb^{-1} of e^+p data and about 20 pb^{-1} of e^-p data. The substantial increase of luminosity during the last two years has enabled the extension of the phase space of such measurements to very high four-momentum transfer squared, Q^2, and small x, the Bjorken scaling variable.

With the statistics presently available one becomes sensitive to physics processes with cross sections of the order of 1 pb and therefore searches for possible deviations from the Standard Model (SM) become particularly meaningful.

In the first part of this paper the single and double differential cross section measurements from both collaborations are presented and discussed in the context of the SM. Interpretations of the NC data in terms of Leptoquark production and Contact Interactions are also presented.

In the second section, the results of searches for events with either an isolated electron or a muon together with large missing transverse momentum are presented. The observed rates are compared to the expectations from SM W production. The observation by H1 of an excess of events with a muon with respect to the expectation from SM processes is discussed.

2 Deep Inelastic Scattering at high Q^2

At HERA deep inelastic scattering of 27.5 GeV positrons or electrons on 920 GeV protons (820 GeV up to the end of 1997) has been studied. Inclusive NC and CC single differential and double differential cross sections have been measured as a function of x, the fraction of momentum carried by the struck quark and of Q^2, the virtuality of the exchanged boson. The very high Q^2 domain ($Q^2 \sim M_Z^2$) is of particular interest as electroweak effects due to Z boson exchange become sizeable in NC processes. Furthermore, the flavour dependence of the NC and CC interactions in the high x and high Q^2 range allows extraction of quark densities.

The data presented here have been accumulated in the period 1994 to 1999. In e^+p collisions data corresponding to an integrated luminosity of ~ 37 pb^{-1} (48 pb^{-1}) were collected by H1 [1] (ZEUS [2, 3]) at a centre of mass (c.m.) energy $\sqrt{s} = 300$ GeV between 1994 and 1997 [1]. In the e^-p mode integrated luminosities of 18 pb^{-1} and 16 pb^{-1} were accumulated at $\sqrt{s} = 320$ GeV by H1 [4] and ZEUS [5, 6] respectively. All measured cross sections presented here are corrected for QED radiation effects.

[1] a further ~ 50 pb^{-1} accumulated by both experiments in the late 1999 to 2000 period, at $\sqrt{s} = 320$ GeV is not included here, with the exception of chap. 5 where the newly collected luminosity is partly used.

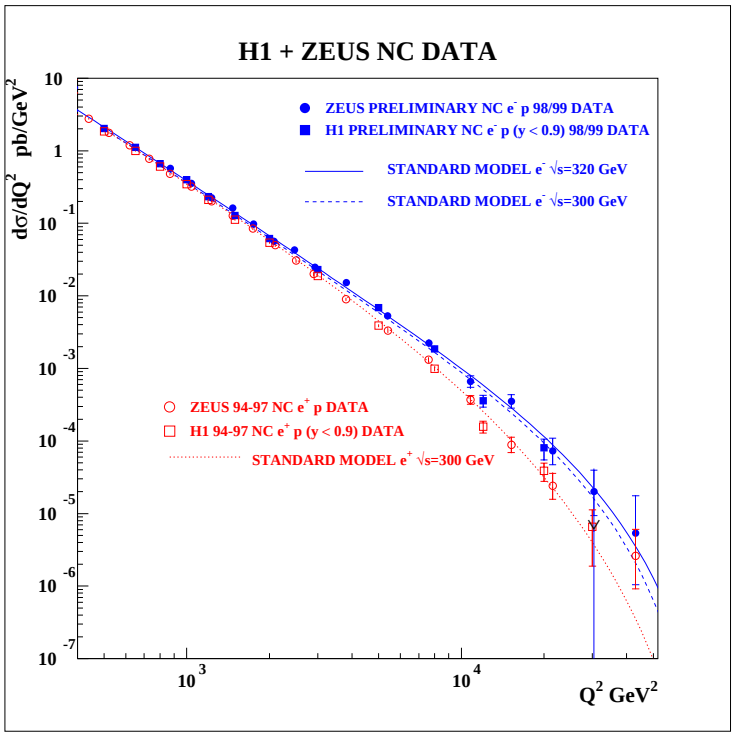

Figure 1: e^+p and e^-p NC cross-sections measured by H1 and ZEUS

3 Neutral Currents

The main signature of NC processes is a scattered electron and a hadronic final state balanced in transverse momentum. The event kinematics can be derived from the measurement of the electron energy and angle θ_e, or from θ_e and the angle of the hadronic final state. H1 uses the electron quantities whereas ZEUS uses the double angle method, each experiment using the other method as a cross check.

3.1 Inclusive cross section

The NC double differential cross section for $e^{\pm}$-p collisions is given by :

$$\frac{d^2\sigma^{\pm}_{NC_{Born}}}{dxdQ^2} = \frac{2\pi\alpha^2}{xQ^4}(Y_+\tilde{F}_2(x,Q^2) - y^2\tilde{F}_L(x,Q^2) \mp Y_-x\tilde{F}_3(x,Q^2)) \quad (1)$$

where α is the fine structure constant, y is the inelasticity of the interaction (Q^2=xys) and $Y_{\pm} = 1 \pm (1-y)^2$ reflects the helicity dependence of the electroweak interactions. The generalised structure function $\tilde{F}_2$ provides the main contribution to the NC cross section. It includes terms accounting for γ and Z^0 exchange, the latter becoming important at high Q^2. The $x\tilde{F}_3$ contribution changes sign according to the incident lepton polarity and becomes significant at high Q^2.

Fig. 1 shows the NC single differential cross section $d\sigma/dQ^2$ measured by H1 and ZEUS for both e^+p ($\sqrt{s}$=300 GeV) and e^-p ($\sqrt{s}$=320 GeV) collisions. The data agree within errors over a wide Q^2 range with the SM predictions. The cross section drops by about 7 orders of magnitude over the 2 orders spanned in Q^2. At $Q^2 \leq 2000$ GeV^2 there is only a small difference between the e^+p and e^-p measurements, mainly due to the increased c.m. energy of the e^-p data which increases the cross section by about 7 %. For $Q^2 > 2000$ GeV^2 the e^-p cross section becomes systematically larger than the e^+p one. This effect is well explained by the SM through the contribution of the γ-Z^0 interference which is constructive (destructive) in e^-p (e^+p) collisions.

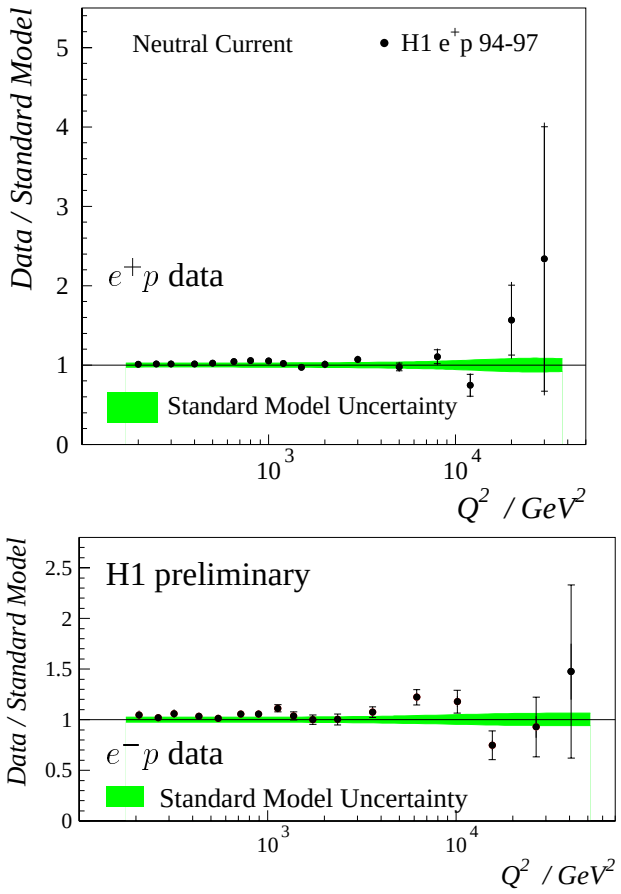

Figure 2: Ratios of NC data compared to SM prediction

The nice agreement between the H1 e^+p and e^-p cross sections and the expectation of the SM is shown in fig. 2. The present level of statistical accuracy at high Q^2 for the e^+p data should improve with the data taken in 1999 and 2000.

Removing the photon propagator factor which contains the dominant part of the Q^2 dependence of the cross section, one obtains the more convenient *reduced cross section* defined as :

$$\tilde{\sigma}_{NC} = x \frac{Q^4}{2\pi\alpha^2 Y_+} \frac{d^2\sigma^{NC}}{dxdQ^2} \tag{2}$$

The H1 measurements of $\tilde{\sigma}^{\pm}_{NC}$ are shown in fig. 3, including BCDMS and NMC fixed target data.

A NLO QCD fit [1], including the e^+p measurement presented here together with lower Q^2 data and data from fixed target experiments, has been performed and gives a good description of the $\tilde{\sigma}^+_{NC}$ measurements as can be seen in fig. 3 (full curves). At x=0.4 and for the highest Q^2 the slight enhancement of the measured cross section over the SM expectation is mainly due to events already reported with the 1994-1996 data [7]. At x=0.65, the QCD fit overestimates the measurement, but the statistical uncertainty of the measurement is here quite large. The corresponding SM expectations for $\tilde{\sigma}^-_{NC}$ (dashed curve) obtained when using for the parton densities those resulting from this QCD fit, are also in good agreement with the e^-p measurements.

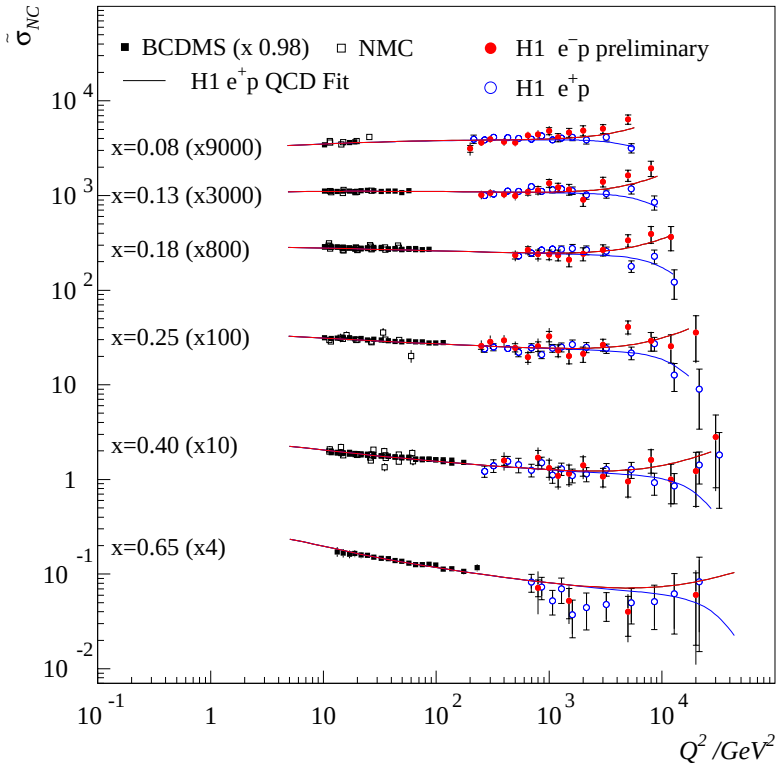

Figure 3: Reduced e^+p and e^-p cross-sections for various fixed values of x.

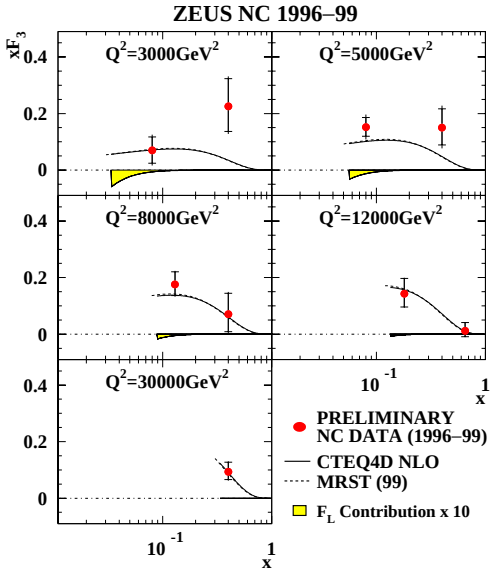

Figure 4: ZEUS results for $x\tilde{F}_3$ at fixed Q^2.

3.2 Measurement of xF_3

Equation 1 shows that the $x\tilde{F}_3$ term enters the cross section with opposite sign, according to the charge sign of the incident lepton beam. Therefore, after appropriately rebinning the e^+p and e^-p reduced cross sections and applying a factor to take into account the influence of the different proton beam energy (820 GeV and 920 GeV) on the $Y_\pm$ helicity function, $x\tilde{F}_3$ can be evaluated using the equation

$$x\tilde{F}_3 = \left(\frac{Y_-^{820}}{Y_+^{820}} + \frac{Y_-^{920}}{Y_+^{920}}\right)^{-1} \cdot \left(\frac{1}{Y_+^{920}} \cdot \tilde{\sigma^-} - \frac{1}{Y_+^{820}} \cdot \tilde{\sigma^+}\right) \quad (3)$$

The contribution of $\tilde{F}_L$ was found to be here negligible and is not taken into account in the extraction of $x\tilde{F}_3$. The results obtained by the ZEUS collaboration [6] are shown in fig 4. These measurements, the first for $x\tilde{F}_3$ in the very high Q^2 domain, are in good agreement with NLO QCD. A similar preliminary analysis by H1 has been presented at ICHEP 2000 [4].

3.3 Constraints on Contact Interactions

The NC high Q^2 data presented above can be used to set constraints on models extending the SM by $eeqq$ contact interactions (CI). Such CI terms can be used to parameterize any new physics process appearing at an energy scale Λ much above the centre of mass energy. At HERA, $eeqq$ four-fermions interactions would interfere (constructively or destructively) with the SM DIS, such that the differential cross sections, e.g. $\mathrm{d}\sigma/\mathrm{d}Q^2$, would be affected.

The H1 [8] and ZEUS [9] Collaborations studied such distortions in e^+p NC data at high Q^2 by performing respectively a χ^2 fit of the single differential cross-section $\mathrm{d}\sigma/\mathrm{d}Q^2$, and a 2-dimensional likelihood analysis in (x, y). H1 further combined the e^+p and the e^-p data recently [10]. Various models (characterizing the chiral structure of the CI) have been constrained and the resulting lower bounds on the scale Λ are depicted in fig. 5, for both relative signs $\varepsilon = \pm 1$ of the DIS and CI contributions. These range between 1.5 and 6.4 TeV and are competitive with the corresponding bounds obtained at the LEP [2] and TeVatron colliders.

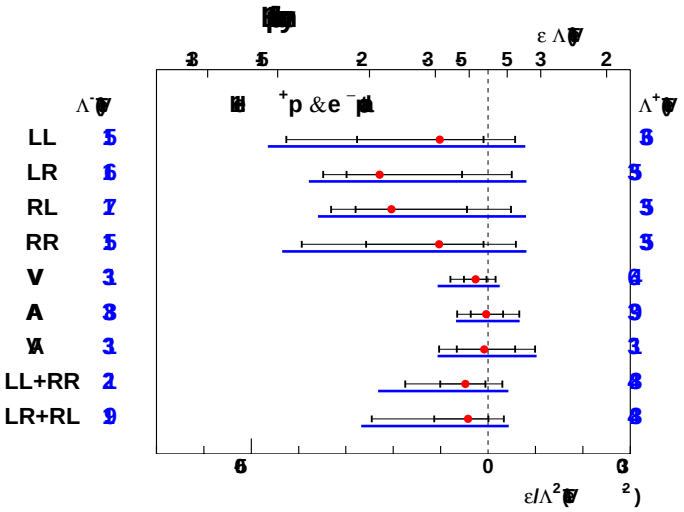

Figure 5: Limits for compositeness models. For various CI models, the thick horizontal bars indicate the 95% lower limits on the scale Λ^+ or Λ^-. The notation on the left refers to the chiral structure of the interaction.

[2] Note that the limits presented here do not rely on the flavour symmetry hypothesis, in contrast to the more stringent bounds obtained at LEP.

3.4 Leptoquarks

Leptoquarks (LQs) are scalar or vector color-triplet bosons, carrying both lepton (L) and baryon (B) numbers, which appear in many extensions of the SM. At HERA, LQs with fermion number $F = 3B+L = 0$ ($F = -2$) could be resonantly produced via a fusion between the incoming positron and a quark (antiquark) coming from the proton. When the LQ decays into $e + q$, the signal would manifest itself as an excess of high Q^2 NC DIS-like events at high y. The H1 [11, 12] and ZEUS [13, 14] experiments used the $e^{\pm}p$ data presented above to search for such LQs. No significant deviation from the SM has been observed, apart from a slight excess in the H1 e^+p data for invariant masses around 200 GeV, mainly due to events previously reported in the 1994-1996 data. A preliminary analysis of the H1 e^+p data taken in 1999-2000 does however not confirm this mass "clustering" [15].

Using a specific theoretical framework [16] in which the the branching ratio β_e of the LQ to decay into $e + q$ is known, mass-dependent limits on the Yukawa coupling λ of the LQ to the $e - q$ pair have been derived. An example of such obtained constraints is shown in fig 6. It can be seen that these limits nicely complement those obtained at other colliders. Conversely, mass dependent limits on the branching β_e have been obtained by H1 and ZEUS, for fixed values of the coupling λ.

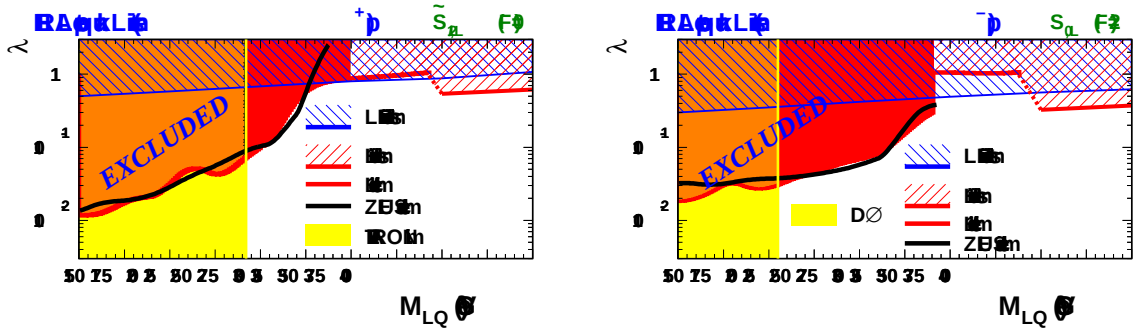

Figure 6: Mass-dependent upper bounds on the coupling λ for a $F = 0$ LQ (left) and a $F = 2$ LQ (right) decaying into eq and νq with an equal branching ratio of 50 %. Greyed and hatched domains are excluded.

4 Charged Currents

In the SM the charged current DIS process is mediated by the exchange of a W boson. The event signature is a hadronic system and missing transverse momentum due to the escaping neutrino. The kinematics can only be derived from the measured energy and angle of the hadronic system.

4.1 Inclusive CC cross section

The CC double differential cross section for e^+p collisions is :

$$\frac{d^2\sigma^+_{CC}}{dxdQ^2} = \frac{G_F^2}{2\pi}\left(\frac{M_W^2}{M_W^2+Q^2}\right)^2\left(\overline{u}+\overline{c}+(1-y)^2(d+s)\right) \tag{4}$$

with the equivalent one for e^-p collisions

$$\frac{d^2\sigma^-_{CC}}{dxdQ^2} = \frac{G_F^2}{2\pi}\left(\frac{M_W^2}{M_W^2+Q^2}\right)^2\left(u+c+(1-y)^2(\overline{d}+\overline{s})\right) \tag{5}$$

where u,d,s,c are the quark densities in the proton. In contrast to NC interactions, where all quark flavours contribute, only up-type (down-type) quarks participate at leading order in e^-p (e^+p) CC DIS

reactions. Hence, σ_{CC} (σ_{NC}) is mainly sensitive to the density $d(x)$ ($u(x)$) at high x. This makes the latter a powerful tool for the flavour specific investigation of the parton momentum distributions.

Fig. 7 shows the CC single differential cross section $\mathrm{d}\sigma/\mathrm{d}Q^2$ measured by ZEUS for both e^+p and e^-p interactions. As expected from the above formula, σ^-_{CC} is much larger than σ^+_{CC}. The data agree within errors over a wide Q^2 range with the SM prediction. Also shown in this figure is the comparison between NC and CC single differential cross sections.

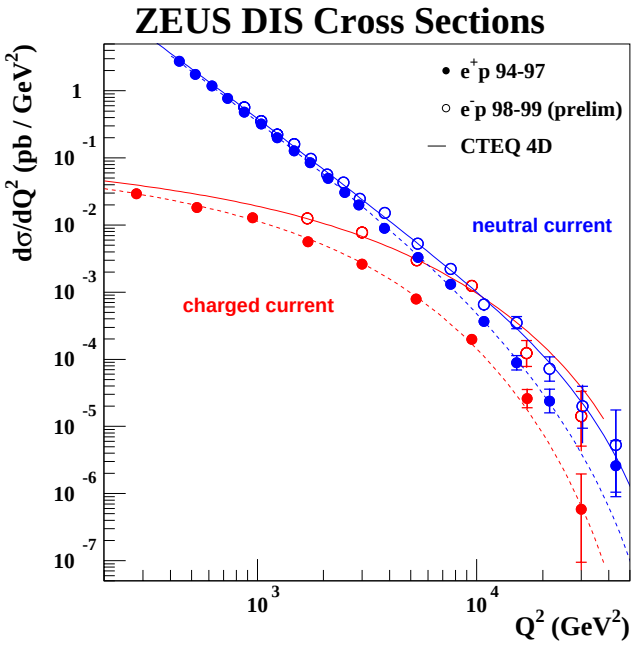

Figure 7: e^+p and e^-p NC and CC cross-sections measured by ZEUS

For $Q^2 > \sim 10000$ GeV^2 they are of equal magnitude, indicating *electroweak unification* at large Q^2 where the effect of the photon propagator is reduced. The e^-p data are well suited for this comparison because both NC and CC currents couple predominantly to the u valence quark in the proton.

4.2 Extraction of quark density functions at high Q^2

As is clear from equation 4, the measurement of $\mathrm{d}^2\sigma^+_{CC}/\mathrm{d}x\mathrm{d}Q^2$ provides information on the density $d(x)$ in a very sensitive manner. Complemented by the precise measurement from the NC $\mathrm{d}^2\sigma^+_{NC}/\mathrm{d}x\mathrm{d}Q^2$, which is mainly driven by the u density, both quark densities can be extracted in a combined parton analysis.

The resulting quark densities are shown in fig. 8 as a function of Q^2 in two x bins. They are in good agreement with the SM expectation obtained from a QCD fit of low Q^2 (< 200 GeV^2) independent data [1].

4.3 Determination of M_W

Fitting the Q^2 dependence of the CC differential cross section one obtains the propagator mass, M_W, which has been determined by H1 and ZEUS, for G_F fixed to its PDG value :

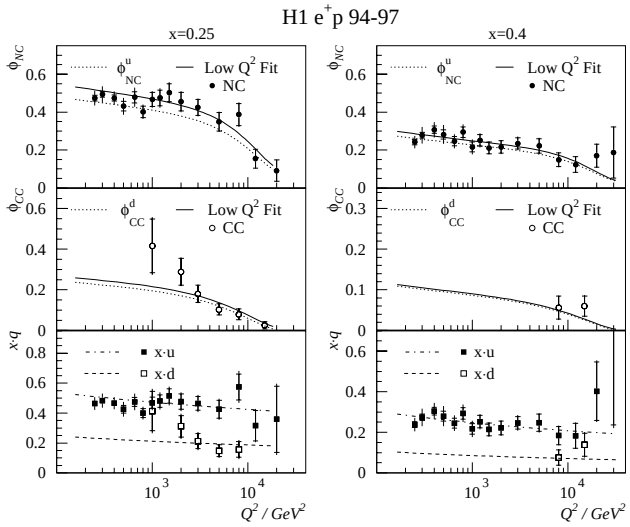

Figure 8: Structure function terms, Φ^+_{NC} and Φ^+_{CC}, and u and d quark densities compared to predictions from NLO QCD. $\Phi^+_{NC,CC}$ is the linear combination of flavour dependent parton densities entering the expression of $\mathrm{d}^2\sigma^+_{NC,CC}/\mathrm{d}x\mathrm{d}Q^2$.

$$M_{prop} = \begin{cases} 80.9 \pm 3.3(stat) \pm 1.7(syst) \pm 3.7(pdf) & \text{H1 [1]} \\ 81.4^{+2.7}_{-2.6}(stat) \pm 2.0(syst)^{+3.3}_{-3.0}(pdf) & \text{ZEUS [3]} \end{cases}$$

These *indirect* determinations of M_W in the space-like domain are in good agreement with the *direct* determinations in the time-like region, such as those done at LEP and TeVatron. This represents an important test of the consistency within the SM.

5 Isolated Leptons

The observation by H1 [17] and ZEUS [18], in the 94-97 e^+p data, of events with an isolated lepton and large missing transverse momentum, a topology typical of the $\ell\nu$ final states for W production, has triggered a lot of interest at HERA. In particular, a few events observed by H1 showed abnormally large values of the hadronic transverse momentum P_T^X. Preliminary results including more recent data [3] are presented here [19, 20]. The selection of W candidates is done by requiring missing transverse momentum and a high P_T track. In both analyses lepton identification (e or μ) is required in addition, H1 applying a further set of cuts against SM processes other than W production. Furthermore, the standard H1 and ZEUS analyses differ in angular acceptance of tracks.

Fig. 9 shows the distribution of P_T^X, the transverse momentum of the hadronic final state of the events with an isolated muon (ZEUS) and of those with an isolated lepton (H1), using for ZEUS (H1) the $e^{\pm}p$ data taken in 1994-1999 (the e^+p data taken in 1994-2000). Both samples correspond to 82 pb^{-1}.

Table 1 shows the comparison [19, 20] between the number of observed events and the SM expectation for both analyses, where the selection criteria have been tightened so that both analyses correspond to a similar set of cuts. The main messages are that the SM expectations are similar for H1 and ZEUS and that H1 sees an excess of events for $\mathrm{P}_T^X > 25$ GeV. Possible interpretations for the H1 events marginally fitting the SM W production topology could include production and decay of supersymmetric particles [21] or anomalous single top production [20, 22].

[3] The results presented here give the status of the H1 and ZEUS analyses shown at ICHEP2000

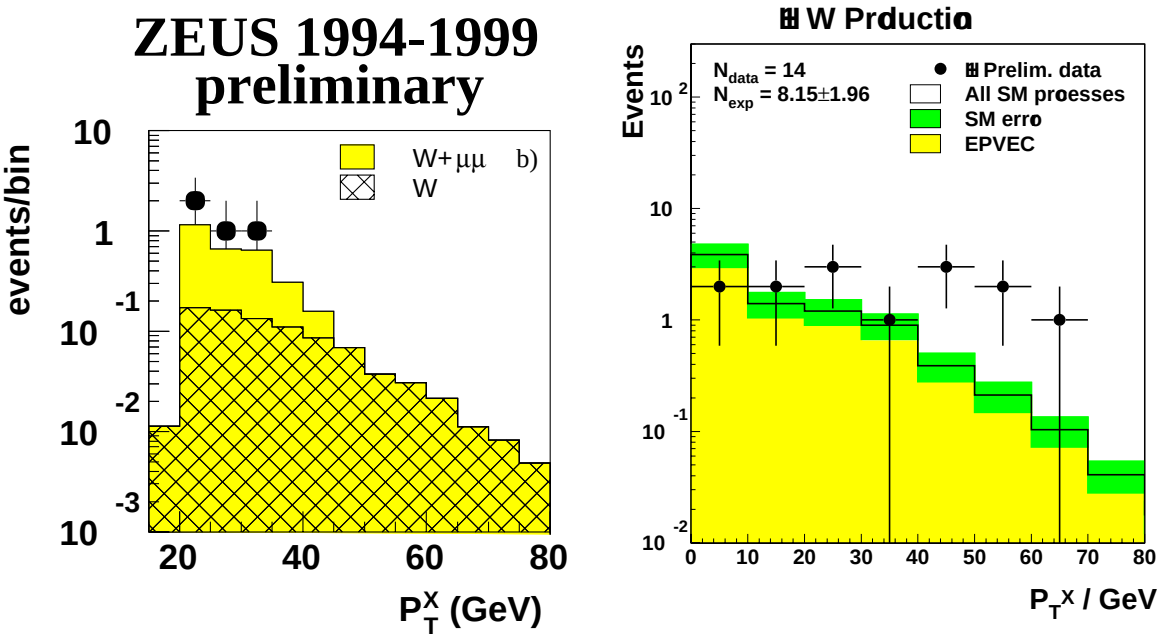

Figure 9: Distribution of P_T^X of the ZEUS and H1 events, compared with the standard Model expectation. In the left(right) figure, the hatched (light shaded) histogram indicates the contribution of W production alone.

Table 1: Number of observed events vs expectation from all SM processes. The standard set of cuts applied by H1 [19] and ZEUS [20] have been tightened so that both analyses can be compared.

$82\ \mathrm{pb}^{-1}$	**H1 94-00 Preliminary** e^+p		**ZEUS 94-99 Preliminary** $e^\pm p$	
	Electrons	Muons	Electrons	Muons
	DATA / SM	DATA / SM	DATA / SM	DATA / SM
$P_T^X > 25$ GeV	3 / 0.84 ±0.22	6 / 0.94±0.26	1 / 0.78	0 / 0.82

Acknowledgments

I wish to thank the organisers for a very enjoyable conference. I am much indebted to my H1 and ZEUS colleagues for their invaluable assistance in helping me prepare this talk and thank them warmly, in particular E. Perez.

References

[1] H1 Collab., C. Adloff *et al.*,*Eur. Phys. J.* C13 (2000) 609.

[2] ZEUS Collab., J. Breitweg *et al.*, *Eur. Phys. J.* C11 (1999) 427.

[3] ZEUS Collab., J. Breitweg *et al.*, *Eur. Phys. J.* C12 (2000) 411.

[4] H1 Collab., Contributed paper #306, ICHEP2000, Osaka, Japan (July 2000).

[5] ZEUS Collab., Contributed paper #414, ICHEP2000, Osaka, Japan (July 2000).

[6] ZEUS Collab., Contributed paper #413, ICHEP2000, Osaka, Japan (July 2000).

[7] H1 Collab., C. Adloff *et al.*, *Z. Phys* C74 (1997) 191.

[8] H1 Collab., DESY-00-027, accepted by *Phys. Lett. B* (2000).

[9] ZEUS Collab., J. Breitweg *et al.*, *Eur. Phys. J.* C14 (2000) 239.

[10] H1 Collab., Contributed paper #305, ICHEP2000, Osaka, Japan (July 2000).

[11] H1 Collab., Eur. Phys. J. C11 (1999) 447 ; erratum *Eur. Phys. J.* C14 (2000) 553.

[12] H1 Collab., Contributed paper #323, ICHEP2000, Osaka, Japan (July 2000).

[13] ZEUS Collab., J. Breitweg *et al.*, *Eur. Phys. J.* C16 (2000) 253.
DESY 00-133, submitted to *Phys. Rev.* D.

[14] ZEUS Collab., Contributed paper #552, EPS'99, Tampere, Finland (July 1999).

[15] H1 Collab., Contributed paper #322, ICHEP2000, Osaka, Japan (July 2000).

[16] W. Buchmüller, R. Rückl and D. Wyler, *Phys. Lett.* B191 (1987) 442 ; erratum *Phys. Lett.* B448 (1999) 320.

[17] H1 Collab., C. Adloff *et al.*, *Eur. Phys. J.* C5 (1998) 575.

[18] ZEUS Collab., J. Breitweg *et al.*, *Phys. Lett.* B471 (1999) 411.

[19] H1 Collab., Contributed paper #308, ICHEP2000, Osaka, Japan (July 2000).

[20] ZEUS Collab., Contributed paper #455, ICHEP2000, Osaka, Japan (July 2000).

[21] T. Kon *et al.*, *Mod. Phys. Lett.* A 12 (1997) 3143.

[22] H1 Collab., Contributed paper #327, ICHEP2000, Osaka, Japan (July 2000).